Revista Internacional de Ciencia y Tecnología de la Información Geográfica
International Review of Geographical Information Science and Technology

dos Santos, K. A., Reis, G. C., Ramos Cortes, J. B., Mendes, T. A., Gitirana, G. de F. N., Formiga K. T. M. (2026). Benchmarking low-cost RPA photogrammetry against Terrestrial Laser Scanning for riverbank erosion monitoring. *GeoFocus*, *Revista Internacional de Ciencia y Tecnología de la Información Geográfica* (Articles), 37, 1-16. https://dx.doi.org/10.21138/GF.969

BENCHMARKING LOW-COST RPA PHOTOGRAMMETRY AGAINST TERRESTRIAL LASER SCANNING FOR RIVERBANK EROSION MONITORING

[1a]Kamila Almeida dos Santos, [1b]Guilherme da Cruz dos Reis, [2c]João Batista Ramos Cortes, [2d]Thiago Augusto Mendes, [1e] Gilson de Farias Neves Gitirana Júnior, [1f]Klebber Teodomiro Martins Formiga

[1]Escola de Engenharia Civil e Ambiental. UFG - Universidade Federal de Goiás. Goiânia, GO, 74605-220, Brazil

[2]Instituto Federal de Educação Ciência e Tecnologia de Goiás – IFG. Goiânia, Goiás, GO, 74055-110, Brazil

[1a]kamila_santos@ufg.br, [1b]guilhermereis@ufg.br, [2c]joao.cortes@ifg.edu.br, [2d]thiago.mendes@ifg.edu.br, [1e]gilsongitirana@ufg.br, [1f]klebberformiga@ufg.br

ABSTRACT

Bank erosion in fluvial channels is a natural geomorphic process that can be significantly intensified by anthropogenic disturbances. This study assesses the contribution of bank erosion to morphodynamic changes in an urban channel through the integration of Terrestrial Laser Scanning (TLS) and low-cost Remotely Piloted Aircraft System (RPA) monitoring techniques. Both channel margins were surveyed over an extended temporal interval, enabling the generation of high-resolution Digital Elevation Models (DEMs) and derived Difference of DEMs (DoDs). Data processing was conducted using two vegetation-filtering approaches: a commercial software workflow and a customised MATLAB algorithm. Both methods provided consistent results, although the commercial software demonstrated superior performance in DoD analysis, while the MATLAB algorithm yielded cross-section profiles more comparable to TLS-derived data. Between 2019 and 2021, volumetric changes for Erosion Zone 01 were 13.55 m³ (commercial RPA), 8.32 m³ (MATLAB RPA), and 19.22 m³ (TLS); for Erosion Zone 02, the respective values were 73.22 m³, 84.69 m³, and 4.68 m³. TLS data exhibited greater stability and reliability in elevation measurement, whereas RPA-derived DEMs were more sensitive to variations in surface cover and vegetation density. These findings highlight the complementary potential of TLS and RPA for detailed quantification of bank erosion processes in urban environments.

Keywords: erosion; remotely piloted aircrafts systems; DEM of Difference (D_oD); Terrestrial Laser Scanner (TLS).

Received: 07/03/2026 Accepted: 09/07/2026
Academic Editor: Dr. Joan Cristian Padró
www.geofocus.org

EMPLEO DEL ESCÁNER LÁSER TERRESTRE COMO REFERENCIA PARA LA EVALUACIÓN DEL RENDIMIENTO DE RPAS DE BAJO COSTO

RESUMEN

La erosión de márgenes en canales fluviales es un proceso geomorfológico natural que puede intensificarse considerablemente por actividades antropogénicas. Este estudio analiza la contribución de la erosión de márgenes a los cambios morfodinámicos en un canal urbano mediante la integración de Escaneo Láser Terrestre (TLS) y sistemas de aeronaves pilotadas de forma remota (RPA) de bajo coste. Ambos márgenes fueron monitorizados durante un periodo prolongado, generando Modelos Digitales de Elevación (MDE) de alta resolución y productos derivados (DoD). El procesamiento de datos se realizó mediante dos enfoques de filtrado de vegetación: un flujo de trabajo con software comercial y un algoritmo desarrollado en MATLAB. Ambos métodos ofrecieron resultados coherentes; sin embargo, el software comercial mostró mejor desempeño en el análisis DoD, mientras que el algoritmo de MATLAB produjo perfiles transversales más cercanos a los obtenidos con TLS. Entre 2019 y 2021, los cambios volumétricos en la Zona de Erosión 01 fueron de 13,55 m³ (RPA comercial), 8,32 m³ (RPA MATLAB) y 19,22 m³ (TLS); en la Zona 02, los valores fueron de 73,22 m³, 84,69 m³ y 4,68 m³, respectivamente. Los datos de TLS presentaron mayor estabilidad y precisión en la medición de elevaciones, mientras que los MDE derivados de RPA se mostraron sensibles a la cobertura superficial y a la vegetación. Los resultados evidencian el potencial complementario del TLS y del RPA para la monitorización y cuantificación detallada de la erosión de márgenes en entornos urbanos.

Palabras clave: erosión, sistemas de aeronaves remotamente pilotadas, diferencia de modelos digitales de elevación (DoD), escáner láser terrestre (TLS).

1. Introduction

Soil erosion is key geomorphological process that affects riverbank stability and influences river channel morphology (Duong Thi & Do Minh 2019). Bank erosion contributes to sediment transport and deposition, playing a fundamental role in channel evolution. Although this process occurs naturally, human activities have altered its intensity and spatial distribution, increased sediment production and modifying hydrological dynamics (Zhao *et al.* 2023) with the urban expansion, water erosion has become a significant socio-environmental problem (Bekele *et al.* 2018, Wang *et al.* 2018, Seifollahi-Aghmiuni *et al.* 2022, Anees & Yan 2019) vegetation removal, and soil sealing disrupt sediment transport and runoff processes, intensifying erosive processes that impact fluvial morphology and water quality (Wilkinson 2005, Zaimes *et al.* 2021). Therefore, there are imbalances in the equilibrium of the geomorphological system, resulting in the acceleration and intensification of erosive processes that can cause irreversible damage to the landscape and generate economic losses (Wilkinson 2005).

Monitoring riverbank erosion is necessary to understand geomorphic changes and assess the effects of environmental modifications. Remote sensing technologies, including Terrestrial Laser Scanning (TLS) and Unmanned Aerial Vehicles (RPAs), enable high-resolution topographic data collection for change detection analyses (Westoby *et al.* 2012, Nourbakhsbeidokhti *et al.* 2019, Hayakawa & Obanawa 2020), TLS captures detailed point clouds with millimeter precision but might be limited by cost and need for multiple scanning positions to cover large areas (Cook 2017, Koutalakis *et al.* 2024); RPA photogrammetry allows for rapid data acquisition over extensive regions, improving geomorphological assessments at lower operational cost (Carbonneau & Dietrich 2017, Falip & Del Cogliano 2019). However, RPA-based models are influenced by vegetation cover, camera calibration, and ground control accuracy, which can introduce uncertainties in elevation measurements (de la Cueva *et al.* 2022, Oldenborger *et al.* 2022). Hence, the hypothesis is that RPA photogrammetry can provide results comparable to TLS but with greater sensitivity to vegetation-induced distortions. Despite the increasing use of RPA photogrammetry in geomorphological studies, few works have systematically compared its accuracy with TLS for monitoring riverbank erosion, particularly in environments where vegetation influences topographic data acquisition.

There are a variety of methods to analyse geomorphic changes, and one of the most used is based on the Dem of Difference (DoD), which consists of a multitemporal analysis, comparing pixel-to-pixel terrain modifications; generating new surfaces indicates volumes and changes calculated (Wheaton *et al.* 2010, Williams 2012). This technique is utilised by many researchers to analyse geomorphological changes in deltas (Wagner *et al.* 2017); fluvial areas (Anderson & Pitlick 2014); comparative analyses post-extreme events (Wicherski *et al.* 2017); glacial areas (Azzoni *et al.* 2023); and others.

This study evaluates the performance of RPA-derived Digital Elevation Models (DEMs) compared to TLS-derived DEMs for assessing fluvial erosion in the Brazilian Savanna and its tropical characteristics. For that, the paper aims to (i) analyse the differences between RPA and TLS datasets in detecting erosion and deposition processes, (ii) quantify volumetric changes using multi-temporal DEMs, and (iii) assess the influence of vegetation cover on elevation accuracy.

2. Materials, data and methods

2.1. The case study

The Barreiro Creek is in the southeast region of the municipality of Goiânia, the capital of the state of Goiás, Brazil (Figure 1). The reach monitored by RPA is approximately 500 m long, and the banks monitored by Terrestrial Laser Scanner (TLS) are inserted within this stretch. The research focused on monitoring the bank erosion identified along the Barreiro stream. Since the TLS scanning occurs within a limited radius and multiple scans of each eroded area are required to obtain several scenes with different faces, it was decided to use the TLS point-by-point at the erosion sites. This differs from the RPA, which acquires the entire area in a single pass during each flight. For the monitoring, two erosion sites along the channel banks were selected. In addition to the logistics of movement, which took place within the water body, the banks chosen were those whose surfaces could be easily identified during the RPA flights. The first bank was approximately 5.5 m long and 4.6 m high. The second bank also had a significant length, of 6.04 m, but its height was smaller, at 2.56 m.

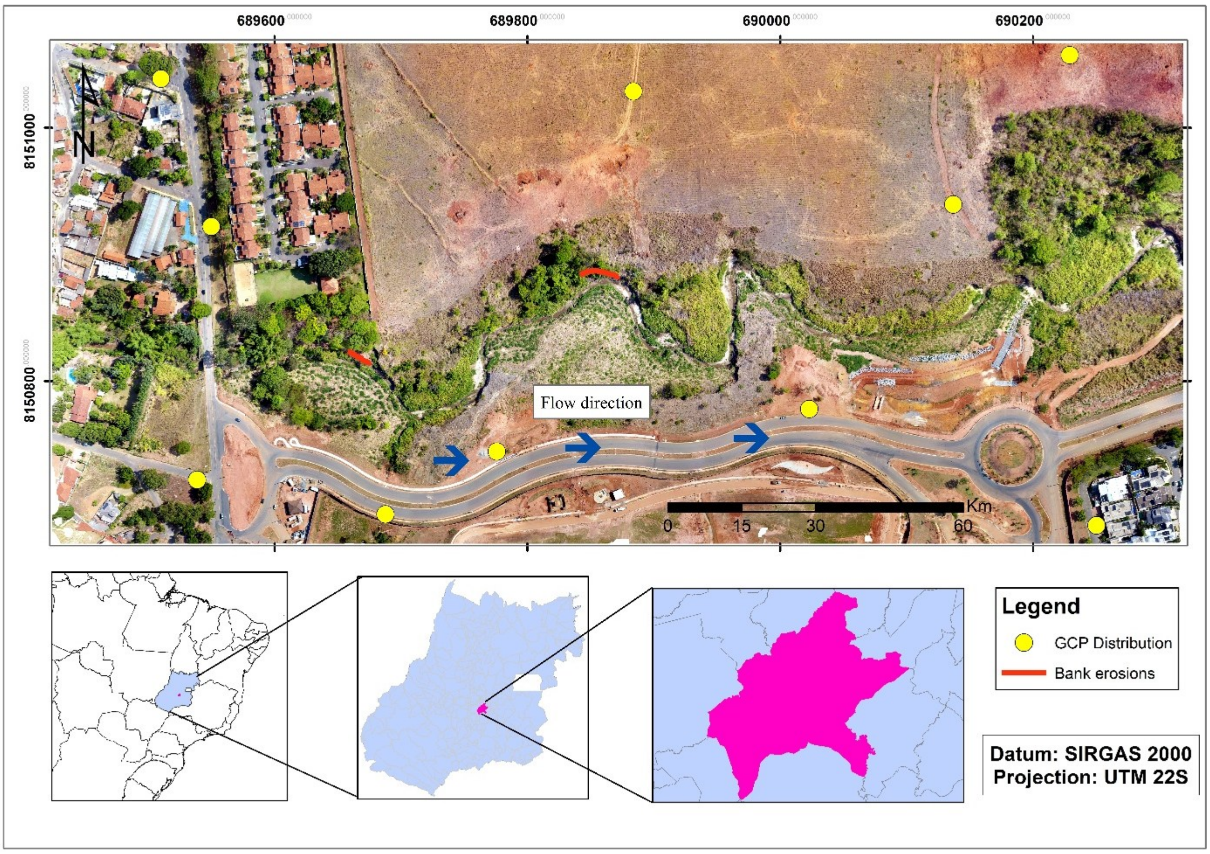

Figure 1. Localisation of the study area

Historically, this area has been used as pastureland, with riparian vegetation removed prior to urban development. The combination of sandy loam soils and reduced vegetation cover has contributed to riverbank instability, thereby modifying channel morphology and influencing sediment transport (Santos *et al.* 2021). Among the remaining native vegetation are forest and grassland formations typical of the Cerrado Biome (Brazilian Savanna), however, along the stream, there are the presence of elephants and colonial grass, an invasive species not native in Brazil that causes various environmental problems and is widely spread in the area (Felfilli *et al.* 2000), consequently, preventing the development of local species essential for maintaining the balance of the local ecosystem. For monitoring, the field campaign for data collection was conducted in September each year (2019 and 2021). Goiânia's climate is Tropical, with two well-defined seasons: a dry season from April to September and a rainy season from October to April.

2.2. Methodological approach and field survey

Terrestrial Laser Scanner data

A Faro Focus 3D X130 Terrestrial Laser Scanner (TLS) was used to monitor the erosive processes on the banks of the Barreiro stream. The TLS scan has 360º horizontal and 270º vertical coverage, with a range of up to 20 meters. The equipment has a ranging error of ±2 mm, defined by the manufacturer as a systematic measurement error at approximately 10 m and 25 m, at one sigma (1σ) (FARO Technologies, 2014). The TLS was always operated on a tripod. TLS is integrated with GNSS (Global Navigation Satellite System), thereby enhancing research precision.

The obtained point clouds had a density of 1 point mm^{-1} and a scan time of approximately 5 min 21 s per laser scan at each position. Initial data processing was performed in the Faro Scene program. This is the most time-consuming step, in which the common geometric relations connecting the scenes (the spheres) are established to perform the joints.

Remotely Piloted Aircraft System- RPA

A DJI Phantom 4 Pro RPA was used throughout the survey campaign, along with a gimbal for connecting the cameras. For the surveys carried out in 2019, a FC6310 camera was used, with an 8.8 mm Charged Coupled Device (CCD) focal length, 5472 x 3648 and a pitch pixel of 2.41 cm. For the 2021 aerial surveys, an FC6310 camera was used with a 3.61 mm focal length, a 4000 x 3000 CCD, and a 1.56 m pitch.

The flights were planned in the Pix4Dcapture application. The aerial survey performed in 2019 had a flight height of 98 m, a Ground Sample Distance (GSD) of 2.5 cm, and a longitudinal and lateral overlap of 80 %. The block consisted of 6 tracks and 161 photographs. The aerial survey performed in 2021 had a flight height of 105 meters, a GSD of 4 cm, and a longitudinal and lateral overlap of 80 %, with the block consisting of 6 tracks and 277 photographs.

As recommended (Aguera-Vega *et al.* 2017, Alves Junior *et al.* 2018, Lima *et al.* 2018), seven Ground Control Points (GCP), were deployed, with 4 targets at the end of the block, 2 in the middle of the outer lanes, and 1 target in the middle of the block, to improve the precision and accuracy of the determination of the internal and external camera orientation parameters. The geometric accuracy of the aerial surveys was assessed through the horizontal and vertical errors obtained during the photogrammetric processing. For the 2019 survey, the vertical and horizontal errors were 0.014 m (1.4 cm) and 0.034 m (3.4 cm), respectively. For the 2021 data survey, the vertical and horizontal errors were 0.033 m (3.3 cm) and 0.135 m (13.5 cm), respectively. These values are consistent with the respective Ground Sample Distances (GSD) of 2.5 cm (2019) and 4 cm (2021), confirming that the geometric quality of the surveys was adequate for the intended analysis.

The GCP model targets contain 4 fins that must pass through the centre of the circle, forming a 90º angle, and their size is determined by the GSD. The three-dimensional coordinates of the pre-signalled targets were determined using a GNSS receiver, using the Real-Time Kinematic (RTK) relative positioning method. The base receiver had a good logging rate and occupancy, and its coordinates were determined by the Precise Point Positioning (PPP) method.

GCPs were manually identified in all photographs following automatic tie-point detection. The point clouds were generated automatically, keeping the default settings. For comparison, the processing of aerial photographs for generating the DEM was carried out in two ways: the first using a commercial program, and the other using a routine written in MATLAB. In both cases, the same DEM obtained by filtering the Digital Surface Model (DSM), eliminating all above-ground objects such as people, vehicles, buildings, and vegetation, leaving only the terrain surface (Ruzgiene *et al.* 2015, Zahawi *et al.* 2015). At the end of processing, all photographs are stitched together to form a single georeferenced orthomosaic.

Geomorphic Change Detection

Using multitemporal DEMs of a study area, one can analyse geomorphology and its volumetric changes, with differences in elevation evaluated at the pixel scale (James *et al.* 2012). The result generated from sequential digital elevation models of the study area is called DEM of Difference (DoD). With this new raster, it is possible to identify and map erosion, deposition, and volumetric changes. The changes in the elevation model can be represented by Equation 1:

$$D_oD = DEM_{new} - DEM_{older} \quad (1)$$

Where DEM_{new} is the latest DEM of the study area, and DEM_{older} is first DEM of the study area.

This subtraction creates a DEM in which positive values represent sedimentation areas and negative values indicate a decrease in terrain elevation, which may be due to erosion. By analysing the altimetry values, it is possible to observe changes that occur. These changes indicate either an increase in soil (a higher altimetric value) or a reduction in soil within the same area (a lower altimetric value).

The results obtained from Equation 1 may be affected by vertical uncertainty of some degree in the DEMs (Wheaton *et al.* 2010, Schwndel *et al.* 2012).

3. Results

Since the erosion features surveyed with RPA and TLS covered areas of different sizes, a polygon shapefile was used as a mask to clip all datasets to a common spatial extent, ensuring a shared local reference. The mask area for Erosion 01 was 114.274 m², and for Erosion 02, 114.273 m². In general, statistical data (Table 1) show good spatial resolution, especially for TLS products; they are more accurate and homogeneous. RPA data presents more variations.

Table 1. general statistics of the two calculated DEM

Data	DEM/Year	Area (m²)	Cell count	Standard Deviation
TLS	E01 - 2019	84.719	10940	1.258
TLS	E01 - 2021	78.148	21002	1.296
TLS	E02 - 2019	73.420	9927	0.962
TLS	E02 - 2021	73.756	14193	0.990
RPA	E01 - 2019	114.266	10970	2.109
RPA	E01 - 2021	114.312	17466	2.520
RPA	E02 - 2019	114.234	10967	1.420
RPA	E02 - 2021	114.312	17466	0.067

The surveyed areas ranged from 73.420 to 84.719 m² for TLS and from 114.234 to 114.312 m² for RPA, indicating a consistently more extensive coverage for the RPA-based surveys. Cell counts ranged from 9,927 to 21,002 for TLS and from 10,967 to 17,466 for RPA. Standard deviation values ranged from 0.962 to 1.296 m for TLS and from 0.067 to 2.520 m for RPA.

DEM of Difference - DoD

The sections of the DoD indicated spatial variation in different elevations. The erosion of the banks suggests soil movement, with some detached layers deposited near the site, creating distinct contours in the area. Different values for DEM_{RPA1} (commercial processing), DEM_{RPA2} (MATLAB routine) and DEM_{TLS} processing, with the class range, where negative values correspond to erosive processes and positive values to sediment deposition.

Area I - Erosion 01

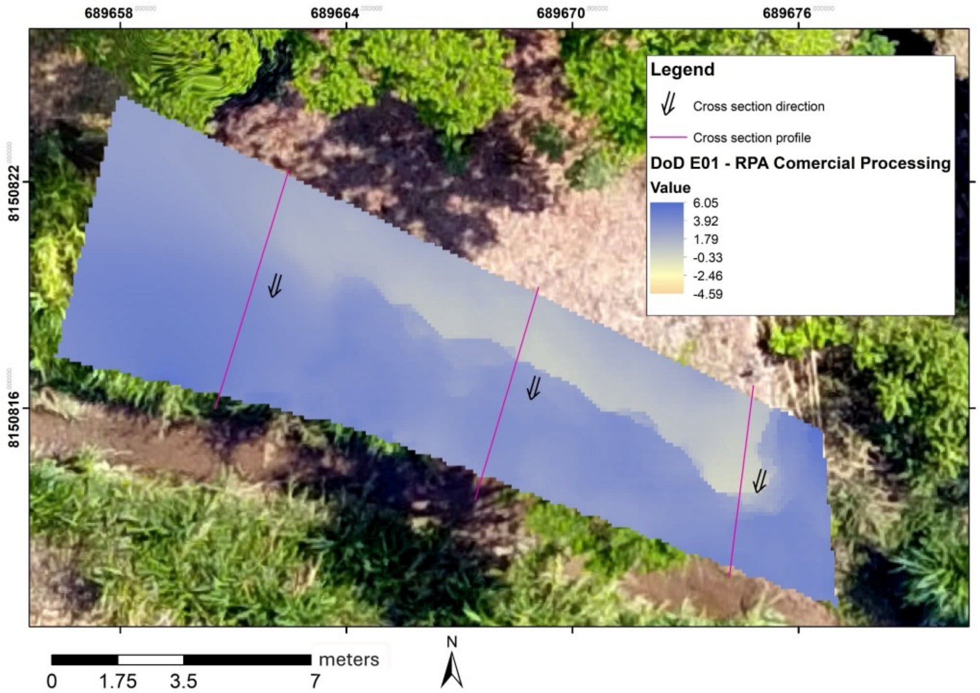

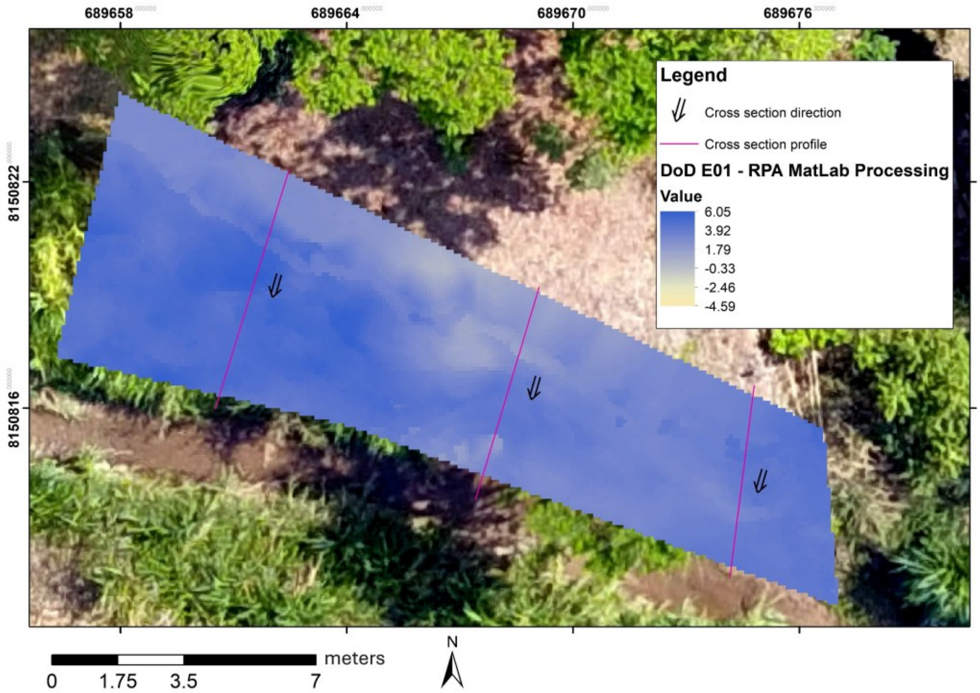

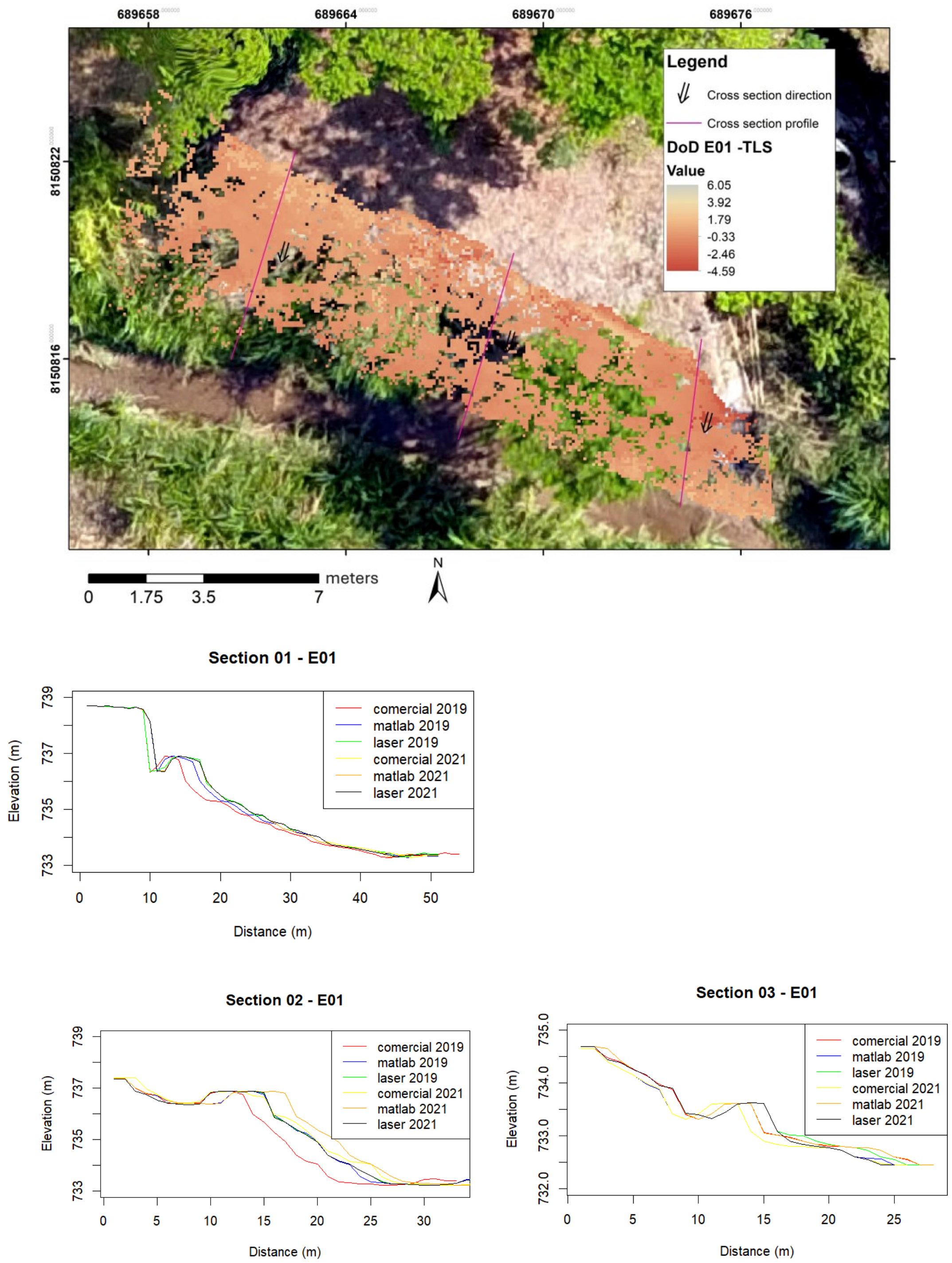

Figure 2. bank erosion in Area 01. 2a - DEM of Difference by RPA using commercial software; 2b - DEM of Difference by RPA using MATLAB processing; 2c - DEM of Difference by TLS; 2d, 2e, 2f – three cross-section profiles comparing the data

Geomorphic Change was detected in different ways through the processes employed in the analysis (Figures 2a, 2b, and 2c). The DoD_{TLS} showed greater variation in erosion and deposition values. In terms of erosion, higher values were observed at the top of the slope, where it is exposed and lacks vegetation cover. The data collected by the RPA and analysed through two distinct processes indicate similar results, with higher positive values indicating greater sediment deposition in the monitored areas.

Three cross-sectional profiles were constructed in E01 (Figure 2d, 2e, 2f), enabling observation of greater alignment among the profiles in section 01. The DEM_{RPA1} section from 2019 started aligned with the others but subsequently followed with its contour below the others. In section 02, the dynamics of the sections diverge, with some profiles spaced apart and others aligned, depending on processing and monitoring dates. In relation to the first two, section 03 shows an intermediate behaviour of the profiles, with some spacing, but all relatively close to each other. In general, the results from DEM_{RPA2} across three sections are more accurate, as these sections are more closely aligned with the DEM_{TLS} sections.

Area II – Erosion 02

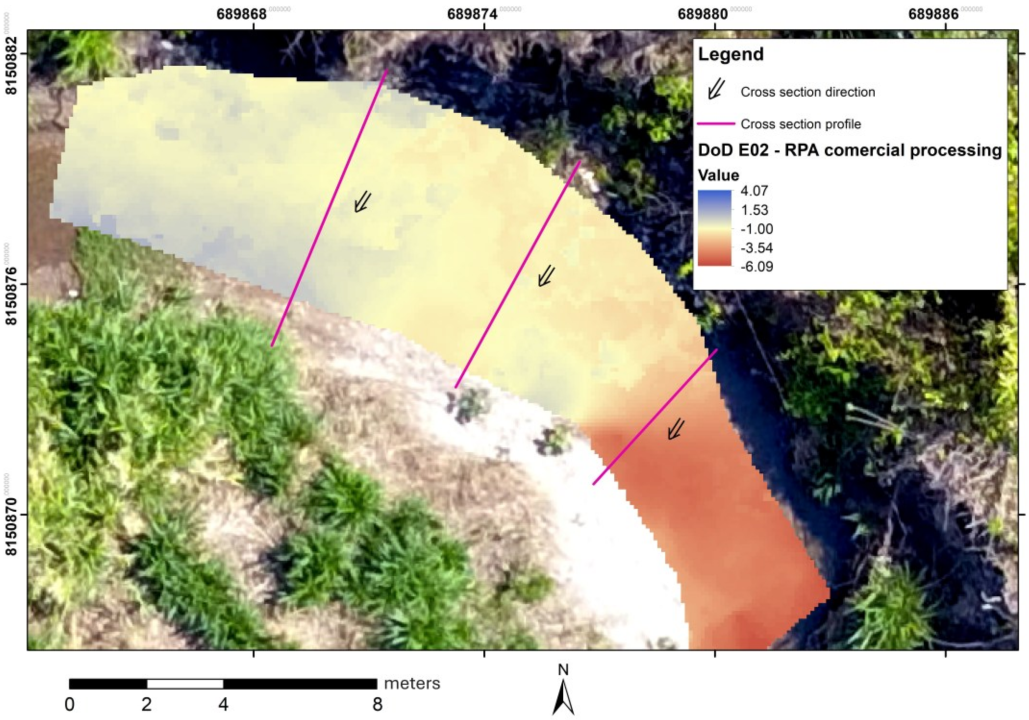

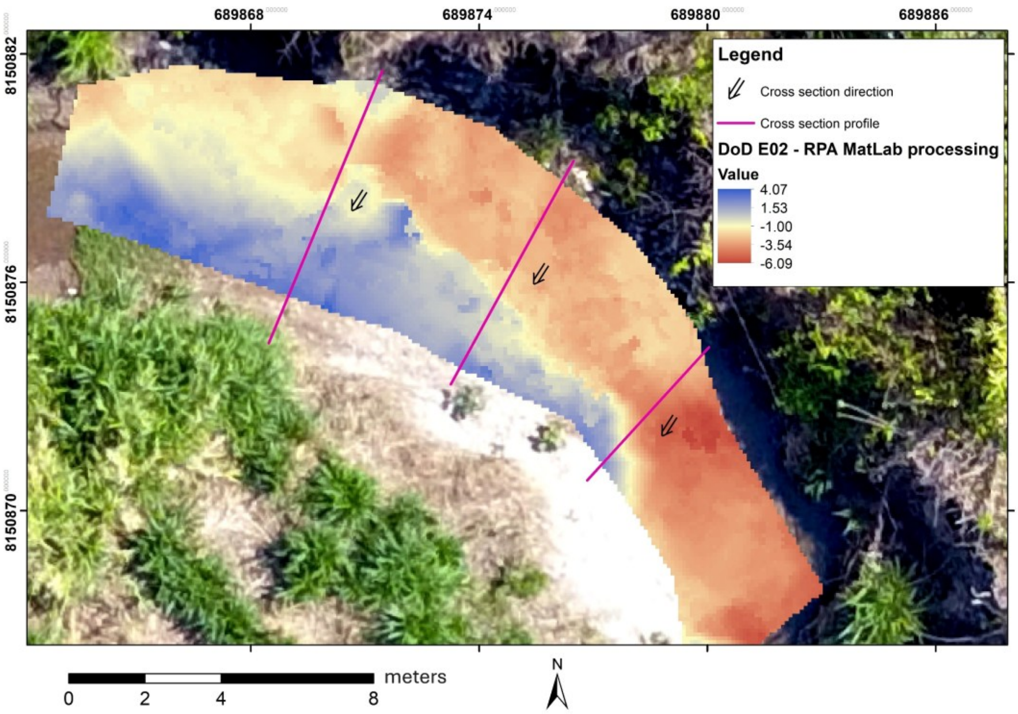

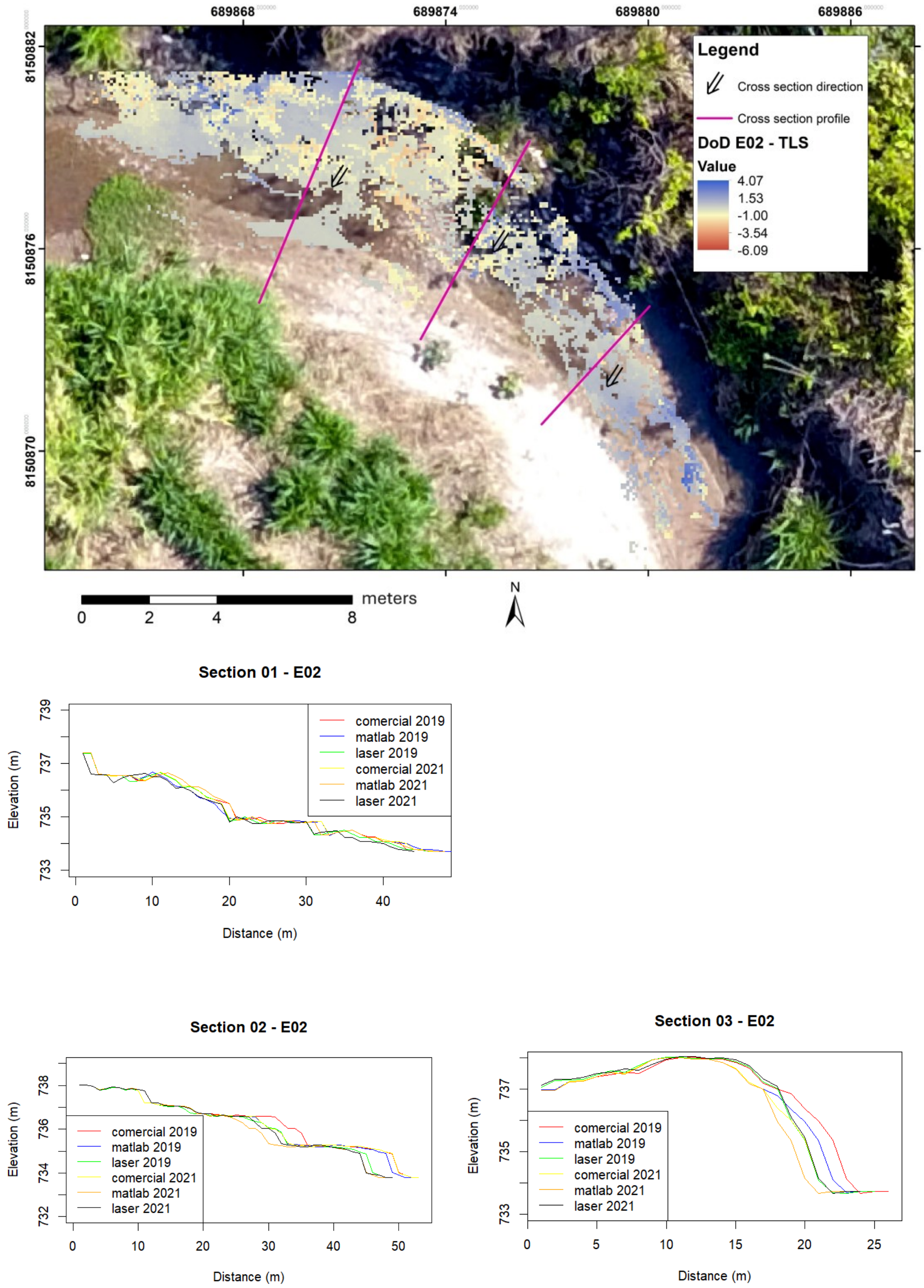

Figure 3. Bank erosion in area 2. 3a - DEM of Difference by RPA using commercial software; 3b - DEM of Difference by RPA using MATLAB processing; 3c - DEM of Difference by TLS; 3d, 3e, 3f – three cross-section profiles comparing the data

The DoDs of E02 (Figure 3a, 3b, 3c) exhibited behaviours similar to those of E01, with DoDRPA1 and DoDRPA2 values close to each other. DoD_{TLS} indicates deposition and erosion along the entire bank of the channel, while DoD_{RPA2} points to erosive processes at the top and middle of the bank, with deposition occurring at the lower part near the channel. DoD_{RPA1} shows a distribution of both processes throughout the bank, with more pronounced negative values at the far end. In the cross-section (Figure

3d, 3e, 3f), the distribution of sediments deposited on the banks varies with bank width and channel length, with different movements observed across the years.

The differences in profile detail across sections reflect the density of vegetation in each monitored section. In Erosion 01 (E01), the bank is cleaner, with grass whose roots are superficial. The E01 is present in a bank with 7.0 meters high with active erosive process, where the predominant granulometry of erosive soils in a place, for these characteristics the erosive process is continuous and accelerated in the E01, the soil that would usually be compacted, when exposed to the erosive process increases the volume due to lateral expansion, because the sandy soil is light and full of gaps that prevent the particles to aggregate.

E02 presents distinct characteristics from E01; besides being smaller, at 4 meters high, it has trees and bushes on site. The soil of E02 is a mixture of silt and clay, with an erosive process different from that of E01, where the moving soil remained in place. Here, the erosive process left the area concave, where the roots of vegetation keep the upper part of the slope in place. The presence of clay and tree roots in E02 contributed to the retention of the soil, a fundamental factor in reducing erosion on the margin.

In general, the plotted profiles appear aligned and exhibit consistent values, with greater spacing observed in section 02 of E01 and section 03 of E02. In the literature, it is possible to find cross-sectional profiles where the DEM RPA and TLS sections aligned almost entirely (Tsunetaka *et al.* 2020), and others where the DEM RPA profiles were completely misaligned with the others (Koci *et al.* 2017).

Volumetric change

The volumetric changes in the monitored areas yielded distinct area and volume values (Table 1) for the same banks.

Table 2. Volumetric changes calculated on monitored areas

Erosion	Data	area 2019	area 2021	Net change area [m²]	volume 2019	volume 2021	Net change volume [m³]
E01	RPAcomercial	110.76	92.69	18,07	369.77	383.12	13,35
E01	laser	68.41	59.46	8,95	130	110.78	19,22
E01	RPA MATLAB	110.85	110.83	0,02	304.22	312.54	8,32
E02	RPA comercial	110.46	90.61	19,85	209.4	136.18	73,22
E02	laser	58.35	61.42	3,07	79.24	83.92	4,68
E02	RPA MATLAB	110.55	110.6	0,05	323.63	238.94	84,69

During the processing of E01 for DEMRPA1, the area decreased by 16.31 %, while the volume increased by 3.61 %. The DEM_{TLS} exhibited a reduction in both area and volume, with decreases of 13.09 % in area and 14.86 % in volume. For DEM_{RPA2}, there was no significant reduction in area (not exceeding 0.1 %), while its volume increased by 2.73 %.

At different levels, all three DEMs showed a reduction in area between the analysed periods; however, only DEM_{TLS} showed a decrease in volume, suggesting the presence of erosive processes. The two processes derived from the RPA indicated an increase in volume, signifying sediment deposition.

In E02, the DEM_{RPA1} experienced a 17.93 % reduction in area and a 34.96 % reduction in volume. The DEM_{TLS} showed a 5.26 % increase in area, accompanied by a 5.91 % increase in sediment deposition. Similar to E01, the area of DEMRPA2 did not change by more than 0.1 %; however, the erosive process accounted for 26.19 % of the displaced volume.

When volumetric change is minimal, errors in cloud registration can occur, interfering with the reading of areas whose altered volumes are small and leading to their undetected (Hayakawa & Obanawa 2020).

Statistical Analysis

A considerable variability was observed between the processing of the two erosions (Figure 4). Among the results for the three products, two of which originated from the same source, significant variations in geomorphic change values were identified across all three processes. Furthermore, it is notable that for the two monitored erosions, the RPA data were closely aligned, indicating that the processing of both successfully yielded some similar results.

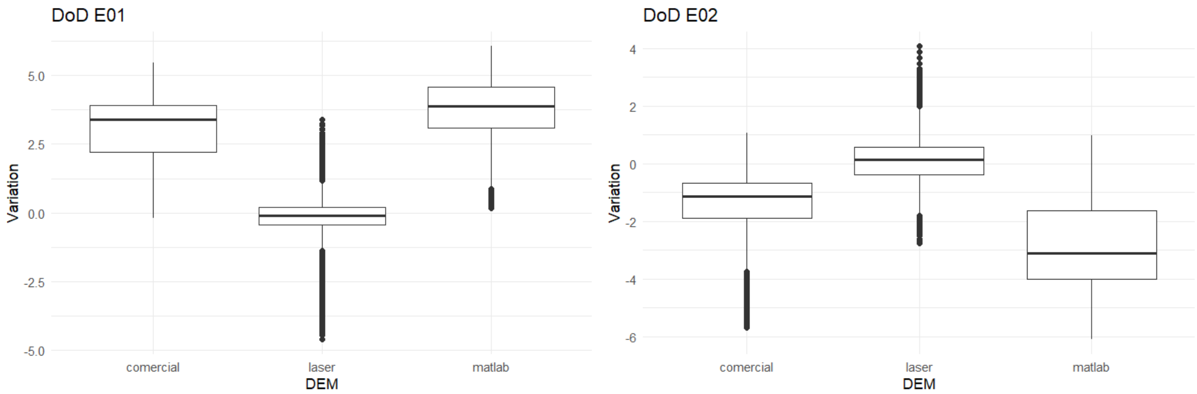

Figure 4. box plot analyzed the variations in the values on the three geomorphic changes products

In E01, DoD_{RPA2} exhibited the greatest difference from the mean (3.77), with a standard deviation of 1.05, indicating moderate data dispersion. DoD_{TLS} had the smallest difference in its values, with a standard deviation of 0.79; however, its mean of 0.07 indicates the influence of outliers and suggests lower variability. Although DoD_{RPA1} had no outliers, its data showed the highest standard deviation (1.15), indicating significant variation in the values and that they are not concentrated near the mean.

While E01 displayed greater variation among the three processes, E02 exhibited less variation, particularly between DoD_{RPA1} and DoD_{TLS}, both of which showed outliers. The standard deviations were 1.54 and 0.91, respectively, while the standard deviation of DoD_{RPA2} was 1.51, indicating higher variability. These values indicate considerable data dispersion, and both DoDRPA1 and DoDRPA2 indicate that many data points are negative. In E01, the influence of trees and vegetation affects the reported values, leading to high mean, median, and maximum values, where as in E02, the indicated volume (Table 1) decreased across the monitored DEMs from 2019 to 2021.

To assess whether the observed differences could be attributed to real morphological changes rather than measurement uncertainty, the RPA's geometric errors were considered. The vertical errors were 0.014 m (2019) and 0.033 m (2021), while the horizontal errors were 0.034 m and 0.135 m, respectively. The error propagation to the vertical component was applied, and the minimum Level of Detection (LoD) at a 95 % confidence level was approximately 0.07 m. Therefore, elevation differences exceeding this threshold can be interpreted as real surface changes, where smaller variations fall within the range of measurement uncertainty and should be interpreted with caution.

4. Discussion

The Barreiro stream exhibits perennial flow, with seasonal flooding occurring between October and March. The morphological characteristics of the banks and the intensity of hydrological events directly influence the erosion process (Santos *et al.* 2021). Flow values in an urban watershed are affected by human activities, which alter the behaviour of the flow regime, especially peak flow (Formiga *et al.* 2016). Flow is one of the main factors in the morphological process; during flood events, erosive forces modify the bank and channel geometry. During the stream monitoring period, seven events with peak flow occurred before the 2019 survey, with an average peak flow of 28.59 $m^3\ s^{-1}$. Before the 2021 monitoring, 13 events were recorded (2020 and 2021), with an average peak flow of 80.64 $m^3\ s^{-1}$. The methodology for determining flow rates was proposed by Reis *et al.* 2020).

Overall, all processing methods could detect erosive processes and sediment deposition in the area, while RPA data presented these data similarly, with values close to each other, but different from those presented by TLS. Furthermore, the TLS DEM showed greater variation in erosion and deposition values compared to RPA data. TLS data presented greater consistency in elevation measurements, while DEMs derived from RPA showed variations influenced by surface coverage. Similar results were reported in previous studies, in which RPA photogrammetry efficiently captured terrain changes but was affected by vegetation and the distribution of ground control points (James *et al.* 2012, Akay *et al.* 2020).

When analysing the DTMs from RPA surveys, the results indicate that the product produced using the MATLAB routine was more accurate and reliable than commercial software. Its cross-sectional profiles showed better alignment with those generated from the TLS DEM.

Geomorphological change detection is an essential tool for validating relief data and assessing sampling variability due to its high sensitivity (Ouédraogo *et al.* 2014). The GCD showed significant changes over a two-year interval. The two sites selected for monitoring in the Barreiro stream represented distinct variations in morphological changes in fluvial dynamics. In the literature, several studies compare RPA and terrestrial or aerial LiDAR data (Tsunetaka *et al.* 2020, Alexiou *et al.* 2021, Kyriou *et al.* 2022). These studies demonstrate that both equipment types enable rapid data acquisition, with LiDAR data validating differences in volume calculations between the two methods (Forlani *et al.* 2018).

In the E01 area, vegetation was sparse, with some clear points and others covered with grass. This allowed the RPA results presented for this location to be more consistent, with values closer to each other. This differs from what occurs in the E02 area, which has denser vegetation with trees and deeper roots, which interfered with data collection and the results presented by RPA products.

The methodological limitations of RPA products primarily concern above-ground characteristics that remain after post-processing. Vegetation was a determining factor in the differences between RPA and TLS data. In E01, where vegetation was less dense, DEMs derived from RPA showed greater correlation with TLS, while in E02, where shrubs and trees were present, RPA models exhibited differences. This occurs because the interpolation used in the process cannot distinguish vegetation from terrain. The discrepancy in areas with denser vegetation suggests that RPA-derived models require additional filtering techniques or post-processing to improve accuracy. Increasing image overlap and reducing flight altitude are strategies that could minimise errors, as indicated in previous studies on RPA photogrammetry (Hamshaw *et al.* 2017).

Despite having less vegetation in E01, the values presented in the DoD were influenced: positive values reached 6.0 m, an unrealistic value for soil movement over a two-year period, while TLS, with outliers present, produced a maximum value of 3.6 m. Additionally, the TLS volume indicates increased erosion, whereas RPA identifies soil deposition in the erosion area. The values from RPA data were close to the range found in TLS DoD; however, once again, vegetation interfered with the results, this time yielding negative values. The area had less vegetation cover in 2021 than in 2019. Even with outliers, TLS results, which were also affected by vegetation, demonstrated a more homogeneous processing approach.

Vegetation is generally present along streams, and its presence interferes with topographic data capture (Alexiou *et al.* 2021, Charters *et al.* 2021). Watercourses in urban environments have higher levels of nutrients, organic matter, and metals that promote plant growth (Yilmaz *et al.* 2018, Silva *et al.* 2023), in addition to those from sewage. Ensuring that debris is absent improves quality, as even small vegetation fragments in high locations can interfere with DEM processing (Hemmelder *et al.* 2018, Du *et al.* 2021). Where trees and shrubs are present, it is difficult to calculate bank changes due to erosion and sediment deposition. Orthomosaics have points significantly obscured by vegetation, introducing uncertainty in volume estimates (Charters *et al.* 2021, Alexiou *et al.* 2024). RPA data collected post-fire exhibited superior spatial resolution compared with data from the period with vegetation cover (Macdonell *et al.* 2023). Despite being in a tropical zone, where vegetation remains present along the watercourse, it may be a limiting factor for photogrammetric data acquisition (Tsunetaka *et al.* 2020, Charters *et al.* 2021). To improve data acquisition in areas with vegetation, it is recommended to increase the overlap percentage and conduct flights at a lower altitude.

The results of this study indicate that low-cost RPA photogrammetry is a potentially viable tool for monitoring riverbank erosion, but its accuracy is influenced by vegetation and terrain complexity. Studies on geomorphological monitoring suggest that integrating multiple remote sensing techniques improves the accuracy of topographic change detection (Koci *et al.* 2017, Reis *et al.* 2020).

5. Conclusions

The research was conducted in an area with limited access, hence the search for remote sensing equipment. Within the Barreiro stream, two locations with different morphological responses and active erosive processes were selected for monitoring. The results indicated that it was possible to estimate the volume and the changes that occurred.

The predominantly sandy soil in the research area, combined with anthropogenic activities, resulted in significant alterations to the channel margins. Considering these alterations, this study aimed to monitor geomorphological changes using low-cost RPAs and compare the data with TLS data. The time series obtained over a two-year interval demonstrated that RPAs and TLS are important assets for monitoring geomorphological processes. Even with good temporal and spatial resolution and the identification of changes on the slope, the results indicate caution in the use of low-cost RPAs, as vegetation directly interfered with the results. For certain surveys, the low-cost RPA can reach a limit in the analysis and processing. When this limit is exceeded and the equipment cannot meet the demands, it is necessary to seek other solutions. The MATLAB processing showed better results than that performed in commercial software, indicating a path for future investigations into data processing methods.

In an ideal monitoring scenario, the study area should have a clean surface with little or no vegetation. However, this work was conducted in a tropical climate region, where vegetation near water bodies is denser, which interferes with the results collected by the RPA. Therefore, it is important to highlight the differences in climate and biomes, as well as the difficulties present in data acquisition.

6. Acknowledgment

The authors would like to thank CNPq (Conselho Nacional de Desenvolvimento Científico e Tecnológico) for supporting this work through a doctoral research scholarship granted to the first author and a Research Productivity Fellowship (Bolsa de Produtividade em Pesquisa, CNPq Call No. 23/2025) awarded to the fourth author. This research was also supported by the R&D Project "Modelling at Different Scales of Sediments Generation in Erosions and Sediments Input in Hydroelectric Power Plant Reservoirs" (PD-ANEEL 0394-1705/2017), funded by Furnas Centrais Elétricas S.A. and the Brazilian Electricity Regulatory Agency (ANEEL), in cooperation with UFG and UnB.

References

Agüera-Vega, F., Carvajal-Ramírez, F., Martínez-Carricondo, P. (2017). Accuracy of digital surface models and orthophotos derived from unmanned aerial vehicle photogrammetry. *Journal of Surveying Engineering*, *143*(2), 04016025. Doi.org/10.1061/(asce)su.1943-5428.0000206.

Alexiou, S., Deligiannakis, G., Pallikarakis, A., Papanikolaou, I., Psomiadis, E., Reicherter, K. (2021). Comparing high accuracy t-LiDAR and UAV-SfM derived point clouds for geomorphological change detection. *ISPRS international journal of geo-information*, *10*(6), 367. https://www.mdpi.com/2220-9964/10/6/367.

Alexiou, S., Papanikolaou, I., Schneiderwind, S., Kehrle, V., Reicherter, K. (2024). Monitoring and quantifying soil erosion and sedimentation rates in centimeter accuracy using UAV-photogrammetry, GNSS, and t-LiDAR in a post-fire setting. *Remote Sensing*, *16*(5), 802. doi.org/10.3390/rs16050802.

Helm, C., Hassan, M. A., Reid, D. (2020). Characterization of morphological units in a small, forested stream using close-range remotely piloted aircraft imagery. *Earth Surface Dynamics*, *8*(4), 913-929. doi.org/10.5194/esurf-8-913-2020.

Alves Júnior, L. R., Ferreira, M. E., Côrtes, J. B. R., de Castro Jorge, L. A. (2018). High accuracy mapping with cartographic assessment for a fixed-wing remotely piloted aircraft system. *Journal of Applied Remote Sensing*, 12(1), 014003-014003. Doi.org/10.1117/1.JRS.12.014003.

Anderson, S., & Pitlick, J. (2014). Using repeat lidar to estimate sediment transport in a steep stream. *Journal of Geophysical Research: Earth Surface*, 119(3), 621-643. doi.org/10.1002/2013JF002933.

Anees, M., & Yan, W. (2019). An overview about the challenges of urban expansion on environmental health in Pakistan. *Journal of Energy and Environmental Policy Options*, *2*(3), 64-71. https://resdojournals.com/index.php/JEEPO/article/view/93.

Azzoni, R. S., Pelfini, M., Zerboni, A. (2023). Estimating the evolution of a post-little ice age deglaciated alpine valley through the DEM of difference (DoD). *Remote Sensing*, *15*(12), 3190. doi.org/10.3390/rs15123190.

Bekele, B., Wu, W., Legesse, A., Temesgen, H., Yirsaw, E. (2018). Socio-environmental impacts of land use/cover change in Ethiopian Central Rift Valley Lakes Region, East Africa. *Applied Ecology & Environmental Research*, *16*(5). doi.org/10.15666/aeer/1605_66076632.

Carbonneau, P. E., & Dietrich, J. T. (2017). Cost-effective non-metric photogrammetry from consumer-grade sUAS: implications for direct georeferencing of structure from motion photogrammetry. *Earth surface processes and landforms*, 42(3), 473-486. doi.org/10.1002/esp.4012.

Charters, F. J., Cochrane, T. A., O'Sullivan, A. D. (2021). The influence of urban surface type and characteristics on runoff water quality. *Science of The Total Environment*, *755*, 142470. doi.org/10.1016/j.scitotenv.2020.142470.

Cook, K. L. (2017). An evaluation of the effectiveness of low-cost UAVs and structure from motion for geomorphic change detection. *Geomorphology*, 278, 195-208. doi.org/10.1016/j.geomorph.2016.11.009.

de la Cueva, A. V., Pita, F. M., Aulló-Maestro, I. (2022). The effect of flowering stage on distribution modelling performance: A case study of Acacia dealbata using maximum entropy modelling and RPA images. *Forest Systems*, *31*(2), e009-e009. doi.org/10.5424/fs/2022312-18787.

Du, Y., Wan, L., Li, X., Yan, G., Liu, S., Qi, S., Lu, T. (2021). High-precision DEM extraction by region segmentation-based progressive triangulation encryption filtering. *Arabian Journal of Geosciences*, *14*(6), 415. doi.org/10.1007/s12517-021-06635-0.

Duong Thi, T. & Do Minh, D. (2019). Riverbank stability assessment under river water level changes and hydraulic erosion. *Water*, *11*(12), 2598. doi.org/10.3390/w11122598.

Falip, S. & Del Cogliano, D. H. (2019). Generation of 3D point clouds with terrestrial laser scanner: Georeferencing and quality evaluation. doi.org/10.14483/23448393.14542.

FARO Technologies. (2014). Focus3D X 130: Performance specifications. https://knowledge.faro.com/Hardware/Focus/Focus/Performance_Specifications_for_the_Focus3D.

Felfili, J. M., Ribeiro, J. F., Fagg, C. W., Machado, J. W. B. (2000). *Recuperação de matas de galeria* (pp. 45-45). Planaltina: Embrapa Cerrados.

Forlani, G., Dall'Asta, E., Diotri, F., Morra di Cella, U., Roncella, R., Santise, M. (2018). Quality assessment of DSMs produced from UAV flights georeferenced with on-board RTK positioning. *Remote sensing*, *10*(2), 311. doi.org/10.3390/rs10020311.

Formiga, K. T. M., Carvalho, M. D., Silva, K. A., Soares, A. K. (2016). Calibração do Storm Water Management Model (SWMM) utilizando algoritmos evolucionários multiobjetivo. *Engenharia Sanitária e Ambiental*, *21*(04), 697-707. https://doi.org/10.5902/2179460X84083.

Hamshaw, S. D., Bryce, T., Rizzo, D. M., O'Neil-Dunne, J., Frolik, J., Dewoolkar, M. M. (2017). Quantifying streambank movement and topography using unmanned aircraft system photogrammetry with comparison to terrestrial laser scanning. *River research and Applications*, *33*(8), 1354-1367. https://doi.org/10.1002/rra.3183.

Hayakawa, Y. S. & Obanawa, H. (2020). Volumetric change detection in bedrock coastal cliffs using terrestrial laser scanning and UAS-based SfM. *Sensors*, *20*(12), 3403. doi.org/10.3390/s20123403.

Hayakawa, Y. S. & Obanawa, H. (2020, September). Volume Measurement of Coastal Bedrock Erosion Using UAV and TLS. In *IGARSS 2020-2020 IEEE International Geoscience and Remote Sensing Symposium* (pp. 5230-5233). IEEE. 10.1109/IGARSS39084.2020.9323220.

Hemmelder, S., Marra, W., Markies, H., & De Jong, S. M. (2018). Monitoring river morphology & bank erosion using UAV imagery–A case study of the river Buëch, Hautes-Alpes, France. International *Journal of Applied Earth Observation and Geoinformation*, 73, 428-437. doi.org/10.1016/j.jag.2018.07.016.

James, L. A., Hodgson, M. E., Ghoshal, S., & Latiolais, M. M. (2012). Geomorphic change detection using historic maps and DEM differencing: The temporal dimension of geospatial analysis. *Geomorphology,* 137(1), 181-198. doi.org/10.1016/j.geomorph.2010.10.039.

Koci, J., Jarihani, B., Leon, J. X., Sidle, R. C., Wilkinson, S. N., & Bartley, R. (2017). Assessment of UAV and ground-based structure from motion with multi-view stereo photogrammetry in a gullied savanna catchment. *ISPRS International Journal of Geo-Information*, *6*(11), 328. https://doi.org/10.3390/ijgi6110328.

KOUTALAKIS, P., GKIATAS, G., XINOGALOS, M., IAKOVOGLOU, V., KASAPIDIS, I., PAGONIS, G., ZAIMES, G. N. Estimating Stream Bank and Bed Erosion and Deposition with Innovative and Traditional Methods. *Land,* 13(2), 232, 2024. doi.org/10.3390/ijgi6110328.

Kyriou, A., Nikolakopoulos, K. G., Koukouvelas, I. K. (2022). Timely and low-cost remote sensing practices for the assessment of landslide activity in the service of hazard management. *Remote Sensing*, *14*(19), 4745. doi.org/10.3390/rs14194745.

Lima, R. P., Coelho, C., Vinueza, G., Grassi, J. T., Castiglione, L. H. G. (2018). The use of RPAS-Remotely Piloted Aircraft Systems in the topographic mapping for mining. *REM-International Engineering Journal*, *71*(2), 281-287. doi.org/10.1590/0370-44672017710120.

MacDonell, C. J., Williams, R. D., Maniatis, G., Roberts, K., Naylor, M. (2023). Consumer-grade UAV solid-state LiDAR accurately quantifies topography in a vegetated fluvial environment. *Earth Surface Processes and Landforms*, 48(11), 2211-2229. doi.org/10.1002/esp.5608.

Nourbakhshbeidokhti, S., Kinoshita, A. M., Chin, A., Florsheim, J. L. (2019). A workflow to estimate topographic and volumetric changes and errors in channel sedimentation after disturbance. *Remote Sensing*, *11*(5), 586. doi.org/10.3390/rs11050586.

Oldenborger, G. A., Bellehumeur-Génier, O., LeBlanc, A. M., McMartin, I. (2022). Landform mapping, elevation modelling, and thaw subsidence estimation for permafrost terrain using a consumer-grade remotely-piloted aircraft. *Drone Systems and Applications*, *10*(1), 309-329. doi.org/10.1139/dsa-2021-0045.

Ouédraogo, M. M., Degré, A., Debouche, C., Lisein, J. (2014). The evaluation of unmanned aerial system-based photogrammetry and terrestrial laser scanning to generate DEMs of agricultural watersheds. *Geomorphology*, 214, 339-355. doi.org/10.1016/j.geomorph.2014.02.016.

Reis, G. D. C. D., Pereira, T. S. R., Faria, G. S., Formiga, K. T. M. (2020). Analysis of the Uncertainty in Estimates of Manning's Roughness Coefficient and Bed Slope Using GLUE and DREAM. *Water*, *12*(11), 3270. doi.org/10.3390/w12113270.

Ruzgienė, B., Berteška, T., Gečyte, S., Jakubauskienė, E., Aksamitauskas, V. Č. (2015). The surface modelling based on UAV Photogrammetry and qualitative estimation. *Measurement*, *73*, 619-627. doi.org/10.1016/j.measurement.2015.04.018.

Santos, K. A. D., Formiga, K. T. M., Braga, V. S., Faria, K. M. S. D. (2021). Mudanças morfológicas na bacia hidrográfica do Córrego Barreiro ao longo do processo de urbanização, Goiânia-GO. *urbe. Revista Brasileira de Gestão Urbana*, *13*, e20200047. doi.org/10.1590/2175-3369.013.e20200047.

Schwendel, A. C., Fuller, I. C., Death, R. G. (2012). Assessing DEM interpolation methods for effective representation of upland stream morphology for rapid appraisal of bed stability. *River Research and Applications*, *28*(5), 567-584. doi.org/10.1002/rra.1475.

Seifollahi-Aghmiuni, S., Kalantari, Z., Egidi, G., Gaburova, L., Salvati, L. (2022). Urbanisation-driven land degradation and socioeconomic challenges in peri-urban areas: Insights from Southern Europe. *Ambio*, *51*(6), 1446-1458. doi.org/10.1007/s13280-022-01701-7.

a Silva, E. P., Filho, N. R. A., Pereira, J., Martins Formiga, K. T. (2023). Temporal variation and risk assessment of heavy metals and nutrients from water and sediment in a stormwater pond, Brazil. *Water Supply*, *23*(1), 206-221. doi.org/10.2166/ws.2022.441.

Tsunetaka, H., Hotta, N., Hayakawa, Y. S., & Imaizumi, F. (2020). Spatial accuracy assessment of unmanned aerial vehicle-based structures from motion multi-view stereo photogrammetry for geomorphic observations in initiation zones of debris flows, Ohya landslide, Japan. *Progress in Earth and Planetary Science*, *7*(1), 24. doi.org/10.1186/s40645-020-00336-0.

Wagner, W., Lague, D., Mohrig, D., Passalacqua, P., Shaw, J., Moffett, K. (2017). Elevation change and stability on a prograding delta. *Geophysical Research Letters*, 44(4), 1786-1794. doi.org/10.1002/2016GL072070.

Wang, L. Y., Xiao, Y., Rao, E. M., Jiang, L., Xiao, Y., Ouyang, Z. Y. (2018). An assessment of the impact of urbanization on soil erosion in Inner Mongolia. *International journal of environmental research and public health*, *15*(3), 550. doi.org/10.3390/ijerph15030550.

Westoby, M. J., Brasington, J., Glasser, N. F., Hambrey, M. J., Reynolds, J. M. (2012). 'Structure-from-Motion'photogrammetry: A low-cost, effective tool for geoscience applications. *Geomorphology*, 179, 300-314. doi.org/10.1016/j.geomorph.2012.08.021.

Wicherski, W., Dethier, D. P., Ouimet, W. B. (2017). Erosion and channel changes due to extreme flooding in the Fourmile Creek catchment, Colorado. *Geomorphology*, *294*, 87-98. doi.org/10.1016/j.geomorph.2017.03.030.

Wilkinson, B. H. (2005). Humans as geologic agents: A deep-time perspective. *Geology*, *33*(3), 161-164. doi.org/10.1130/G21108.1

Williams, R. (2012). DEMs of difference. *Geomorphological techniques*, *2*(3.2). https://eprints.gla.ac.uk/114527/1/Williams%202012%20DEMs%20of%20Difference.pdf

Wheaton, J. M., Brasington, J., Darby, S. E., Merz, J., Pasternack, G. B., Sear, D., Vericat, D. (2010). Linking geomorphic changes to salmonid habitat at a scale relevant to fish. *River research and applications*, 26(4), 469-486. doi.org/10.1002/rra.1305.

Yilmaz, V., Konakoglu, B., Serifoglu, C., Gungor, O., Gökalp, E. (2018). Image classification-based ground filtering of point clouds extracted from UAV-based aerial photos. Geocarto international, 33(3), 310-320. doi.org/10.1080/10106049.2016.1250825.

Zaimes, G. N., Tamparopoulos, A. E., Tufekcioglu, M., Schultz, R. C. (2021). Understanding stream bank erosion and deposition in Iowa, USA: A seven year study along streams in different regions with different riparian land-uses. *Journal of Environmental Management*, *287*, 112352. doi.org/10.1016/j.jenvman.2021.112352.

Zahawi, R. A., Dandois, J. P., Holl, K. D., Nadwodny, D., Reid, J. L., Ellis, E. C. (2015). Using lightweight unmanned aerial vehicles to monitor tropical forest recovery. *Biological Conservation*, *186*, 287-295. doi.org/10.1016/j.biocon.2015.03.031.

Zhao, L., Meng, P., Zhang, J., Zhang, J., Li, J., Wang, X. (2023). The contribution of human activities to runoff and sediment changes in the Mang River basin of the Loess Plateau, China. *Land Degradation & Development*, 34(1), 28-41. doi.org/10.1002/ldr.4441.